scientific data

OPEN

DATA DESCRIPTOR

Beryllium 10 in Antarctica over the last seven millennia

Jean Jouzel[1] ✉, Alexandre Cauquoin[2], Edouard Bard[3], Li Zhang[4,5], Shugui Hou[6], Zhenkun Wu[4,5], Weijian Zhou[4,5,7], Volodya Lipenkov[8], Jean-Robert Petit[9], Grant Raisbeck[10] & Françoise Yiou[10]

Since the first measurements of beryllium 10 (^{10}Be) in ice, in the seventies, numerous profiles of this cosmogenic isotope have been obtained both in Antarctica and Greenland. In this article, we focus on Antarctic data, available at nine different sites, covering a significant part of the Holocene, from 237 to 7101 yr BP. We show that correlating their ^{10}Be profiles allows to synchronize these ice cores with an excellent accuracy and to document the spatial variability of ^{10}Be concentration and flux. We then examine how this variability is taken into account by a simulation of ^{10}Be fallout recently performed with the ECHAM6.3-HAM2.3 model. Except for a systematic underestimation of ^{10}Be fluxes at high accumulation sites, these simulations are overall very satisfying. Finally the excellent accuracy of synchronisation based on ^{10}Be profiles allows us to derive an Antarctic stack record over the last seven millennia. The reliability of the new ^{10}Be stack is demonstrated by its superior correspondence with the accurately dated IntCal20 record based on ^{14}C in tree rings.

Background & summary

Beryllium 10 (^{10}Be) is a radionuclide (half-life of 1.39 • 10^6 yr[1,2]) formed by the interaction of cosmic rays with the Earth atmosphere and then precipitated out into various geophysical reservoirs such as loess, marine sediment and polar ice[3]. The ^{10}Be flux is modulated by the heliomagnetic and geomagnetic fields[4,5]; the higher these fields are, the more primary cosmic ray particles are deflected which leads to a decrease in cosmogenic isotope production with two consequences. First geomagnetic reversals[6] and, for a shorter period, geomagnetic excursions[7] - both characterized by lower geomagnetic intensity - are associated with ^{10}Be peaks. Second, as there is a relationship between heliomagnetic activity and solar irradiance[8,9], reduced solar activity is associated with increased ^{10}Be production, a relationship which can be used to estimate solar activity. More recently, sharp increases in ^{10}Be[10,11] have been documented at the time of extreme solar particle events discovered from measurements of ^{14}C - a radionuclide also formed by the interaction of cosmic rays with the Earth atmosphere - in trees[12].

Raisbeck *et al.*[13,14] reported the first measurements of cosmogenic ^{10}Be in ice for samples from a 906 m core drilled during the 1977-78 Antarctic field season at the old Dome site, 50 km from the Dome Concordia station. They found a ^{10}Be concentration that was larger in glacial-age ice by a factor of 2 to 3 than in Holocene ice. Among the possible explanations offered was that the precipitation rate in Antarctica during the glacial period was approximately 50% of that during the Holocene. In turn, measuring ^{10}Be in the ice provides useful information about the change of accumulation with time along ice cores as illustrated, in the eighties and nineties, from the Dome C and Vostok deep ice core then extending respectively into the last and previous glacial

[1]Laboratoire des Sciences du Climat et de l'Environnement/Institut Pierre Simon Laplace (LSCE/IPSL CEA-CNRS-UVSQ), Orme des Merisiers, CEA Saclay, 91191, Gif-sur-Yvette, France. [2]Institute of Industrial Science, The University of Tokyo, Kashiwa, Japan. [3]CEREGE, Aix-Marseille University, CNRS, IRD, INRAE, Collège de France, Technopôle de l'Arbois, BP 80, 13545, Aix-en-Provence, France. [4]State Key Laboratory of Loess Science, Institute of Earth Environment, Chinese Academy of Sciences, Xi'an, 710061, China. [5]Shaanxi Key Laboratory of Accelerator Mass Spectrometry (AMS) Technology and Application, Xi'an AMS Center, Xi'an, 710061, China. [6]School of Oceanography (SOO), Shanghai Jiao Tong University (SJTU), 1954 Huashan Road, Xuhui District, Shanghai, China. [7]Interdisciplinary Research Center of Earth Science Frontier, Beijing Normal University, Beijing, 100875, China. [8]Arctic and Antarctic Research Institute, Beringa Street 38, 199397, St. Petersburg, Russia. [9]Institut des Géosciences de l'Environnement (IGE), CNRS-UGA-IRD-GINP, Grenoble, 38402, France. [10]IJCLab, Université Paris-Sud XI, Bât 108, 91405, Orsay, France. ✉e-mail: jean.jouzel@lsce.ipsl.fr

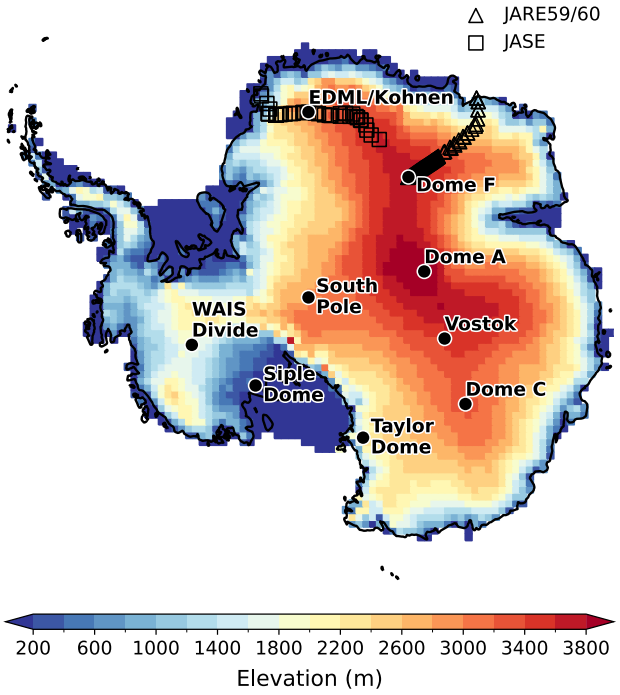

Fig. 1 Map of Antarctica with the 9 sites where ^{10}Be data are available over a part of the Holocene. Colored background indicates the elevation.

periods[7,15–17]; ^{10}Be peaks[7] - characteristic of periods of lower geomagnetic intensity such the one associated with the Laschamps event - were identified at these two sites.

Getting access to solar variability was one of the initial objective of ^{10}Be measurements. Raisbeck *et al.*[14] pointed out to an enhanced ^{10}Be concentration about the time of the Maunder minimum. This enhancement, also observed in Greenland ice cores[18], was confirmed by measurements covering the last millenium at South Pole[19]. That record closely correlated with the ^{14}C measurements obtained on tree rings with periods corresponding to solar activity minima centred at about 1060 (Oort), 1320 (Wolf), 1500 (Sporer), 1690 (Maunder) and 1820 (Dalton) yr A.D.

Since both ^{10}Be and ^{14}C have the same origin (nuclear reactions of cosmic rays in the earth's atmosphere), the idea of synchronizing their profiles, and thus their ages, was rapidly shown to have promise[20,21]. This is particularly important for ice cores from the Antarctic plateau where low ice accumulation rates preclude layer counting. Based on a 180 m core drilled at the old Dome C site, Raisbeck and Yiou[21] discussed the potential of such a comparison for dating Antarctic ice cores. Bard *et al.*[22,23] developed a more quantitative approach by using ^{10}Be in a 127 m dated South Pole core as input to a 12-box carbon cycle model to simulate an atmospheric ^{14}C.

Using a similar approach, Raisbeck *et al.*[24] derived the age for the bottom of the 178 m Vostok BH1 core and concluded that the EGT timescale[24,25] was too young by a gradually increasing amount which, at the bottom of this core, eventually reached ~400 years at 7000 yr BP (before 1950 AD). This study provided an absolute time marker which has later been systematically taken into account for Vostok[26,27] and Antarctic ice core[28] chronologies. While this time marker has thus been used extensively, the ^{10}Be data on which it was based was never published. Doing that was in fact the initial motivation for the present paper.

Beyond this pioneering work, ^{10}Be profiles covering part of the Holocene have now been measured in 9 different Antarctic sites (Fig. 1) with two adjacent ice cores, BH1 and BH2, near the Vostok station, two, PS1 and SPICE, near the South Pole station, three in the Dome C area - one, EPICA Dome C (EDC) near the Dome Concordia station and two, Old Dome C (ODC) and Little Dome C (LDC), respectively 50 and 40 km away - and single ice cores otherwise (Siple Dome, Taylor Dome, Wais Divide, Dome A, Dome F and EDML). Thanks to this ensemble of data, we hereafter document the geographical variability of the ^{10}Be fallout and its relationship with the ^{14}C record over a longer time period, the last ~7 ka. Our study is based on ^{10}Be profiles measured by the Orsay team (who are authors of the present study) for two of the cores drilled in the Dome C area - old Dome C[21] and EPICA Dome C - the two cores drilled at Vostok - BH1 and BH2 - and one, PS1, drilled at South Pole[18]. We also use a profile obtained in collaboration between this team and the Xi'an AMS Center along a core drilled at Dome A[29]. In addition, our study includes profiles obtained by other teams at EDML, WAIS Divide (WD), Siple Dome (SD), Taylor Dome (TD), Dome F (DF), SPICE (SPI) at South Pole and Little Dome C (see below).

We note here a study of Nilsson *et al.*[30] aiming to reconstruct variations in average hemispherical ^{10}Be production rates based on data obtained from both Greenland and Antarctic ice cores over the Holocene. For Antarctica these authors use data from EDML completed by short records from Dome F, Siple Dome and South Pole including a second profile recently measured[31] along the SPICE core retrieved at this site starting ten years ago[32]. Our study is based on a larger ensemble of data with additional profiles at Vostok, Dome A (DA), WAIS

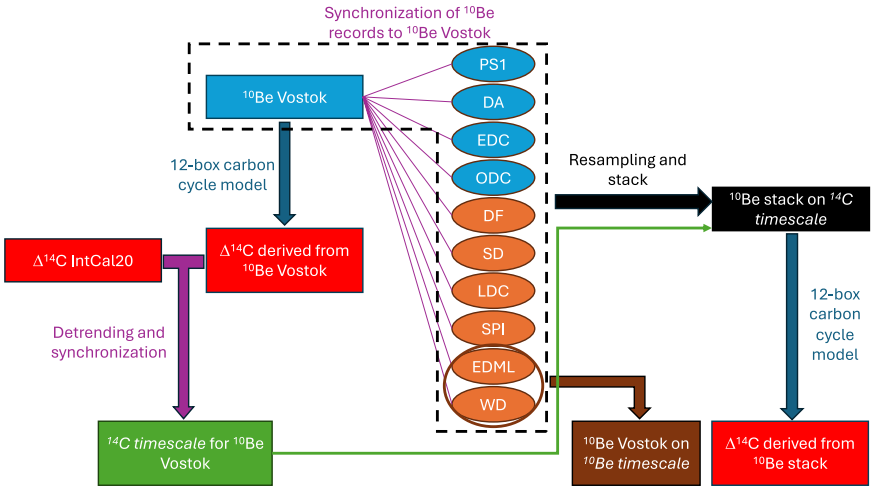

Fig. 2 Flowchart resuming the method used in this study. ^{10}Be ice core data from Orsay team and other teams are in blue and orange, respectively. The acronyms are detailed in Table 1.

Divide and three in the Dome C area which allows us to discuss the geographical variability of the ^{10}Be fallout over Antarctica. For documenting this geographical variability, we account, in addition, for ^{10}Be near surface data available along traverses conducted in the Dronning Maud Land area in the Atlantic sector of East Antarctica (Fig. 1). Near surface data are also available at Law Dome[33].

In this article, we first focus on the use of ^{10}Be profiles as a dating tool comparing two approaches providing independent absolute timescales. First we use the ^{10}Be - ^{14}C correlation through a synchronization on the Δ^{14}C calibration curve IntCal20[34] to derive an absolute timescale as initially suggested by Raisbeck and Yiou[21] and developed by Bard *et al.*[22], and apply it to the continuous and detailed Vostok profile back to ~ 7 ka; this timescale is referred to as the *^{14}C timescale*. Second we synchronize the ice cores on a common relative timescale by correlating their ^{10}Be profiles, except for Taylor Dome and for the lower part of Siple Dome for which data are too sparse. We then derive a second Vostok absolute time scale - referred to as the *^{10}Be timescale* - using the fact that one of the cores, WAIS Divide, is dated by layer counting with a good accuracy[35]. Based on this ^{10}Be synchronization, we then examine the geographical variability of the ^{10}Be fallout over Antarctica and compare this variability with results from a recent simulation of this ^{10}Be fallout using an Atmospheric General Circulation Model (AGCM)[36]. Finally, we propose a ^{10}Be stack for the last 7 ka and a simulated ^{14}C record based on our ^{10}Be stack profile in order to test if this stack better accounts for the solar modulation than individual profiles. The method is resumed in the flowchart in Fig. 2.

Methods

^{10}Be data from old Dome C, South Pole (PS1), Vostok, EPICA Dome C and Dome A. Key characterics of ^{10}Be data used in this study are summarized in Table 1. In Fig. 3 are shown with respect to depth ^{10}Be data measured in the Orsay laboratory (old Dome C[19], PS1[19], Vostok[24] and EPICA Dome C) and at the Xi'an AMS Center (Dome A[29]). EPICA Dome C data have never been published by the authors of the present study, and the other records were used in previous publications, but not available in an open database (see Table 1). Samples from Old Dome C, South Pole (PS1) and Vostok were prepared by the Orsay team using the following analytical procedure. After melting the ice with 500 or 250 µg of ^{9}Be carrier, beryllium was extracted by loading on a Dowex 50W-8X, 200-300 mesh ion exchange column and leached off with HCl. It was then precipitated as $Be(OH)_2$ and transformed into BeO by heating. For EPICA Dome C and Dome A, smaller quantities of ice (~60 g and ~100 g respectively) were used, which permitted direct precipitation of $Be(OH)_2$ without concentrating with the ion exchange resin. The BeO, together with carbon, silver or niobium powder, was pressed into Cu or Mo cathodes in order to measure the ^{10}Be/^{9}Be ratio by accelerator mass spectrometry. Knowing the weight of ice, weight of ^{9}Be and the measured ^{10}Be/^{9}Be, the concentration of ^{10}Be in the ice is calculated relative to the NIST standard for which the nominal ratio ($2.68 \bullet 10^{-11}$) is adopted.

For the old Dome C site, located 50 km from the EPICA Dome C site, a nearly continuous profile has been obtained on the lower part of a 180 m ice core drilled during the 1978-79 field season[37] about 10 m away from the 906 m ice core. About half of the samples from the upper part of the core were initially measured at the Grenoble cyclotron using six times higher ^{9}Be carrier because it was necessary to fabricate self supporting Be pellets[14]. Although these samples were remeasured with the Tandetron, the larger ^{9}Be carrier led to higher uncertainties. For this reason, we limit here the use of this old Dome C profile for the record below 56 m (Fig. 3) which from the dating derived by Raisbeck and Yiou[21] extends between ~1 and 4 ka.

For the 127 m long PS1 core retrieved in 1984 near the South Pole station, measurements were performed using 1 kg samples every 0.8 m on average. This core, which covers slightly more than 1 ka (Figs. 3 and 4), was dated by recognizing 20 layers of impurities attributed to known volcanic eruptions and by correlation with a nearby core for which seasonal variations are observed for major ions and water isotopes[38].

Site	Covering period (yr BP)	Mean time resolution on the synchronization period (years)	Original time scale	Scaling factor applied with respect to NIST standard	Raw data?	Related scientific publications	Data in open access repository before this study?	Licence
Vostok (VK)	234 - 6754	20	EGT[25]	no	yes	This study + Ref.[24]	No. Data produced by the authors of this study.	CC BY 4.0
Dome A (DA)	4 - 3122	23	Ref.[29]	no	yes	This study + Ref.[29]	No. Data produced by the authors of this study.	CC BY 4.0
EPICA Dome C (EDC)	56 - 1031	5	AICC2012[28]	no	yes	This study	No. Data produced by the authors of this study.	CC BY 4.0
Old Dome C (ODC)	1078 - 4338	25	EDC1[86,87]	no	yes	This study + Ref.[19]	No. Data produced by the authors of this study.	CC BY 4.0
PS1 (PS1)	-28.5 - 1103	23	Ref.[38]	no	yes	This study + Ref.[19]	No. Data produced by the authors of this study.	CC BY 4.0
Dome F (DF)	74 - 1251	10	Ref.[49]	0.89	yes	Ref.[48,49]	Yes[53]	CC BY 4.0
EDML (EDML)	1216 - 7134	22	AICC2012[28]	0.91	No	Ref.[45]	Contact with Jürg Beer asking for agreement to deposit the data in the open access repository related to this study.	CC BY 4.0
Little Dome C (LDC)	-69 - 630	9	Ref.[50]	0.96	yes	Ref.[50]	Contact with Long Nguyen asking for agreement to deposit the data in the open access repository related to this study.	CC BY 4.0
Siple Dome (SD)	-44 - beyond 7100 yr BP, but the synchronization could not be made beyond 3568 yr BP.	11	Ref.[88]	no	yes	No	Yes[46]	CC BY-NC 4.0
SPICE (SPI)	66 - 2064	11	SP19[89]	no	yes	No	Yes[31]	CC BY-NC 4.0
Taylor Dome (TD)	-9 - beyond 7100 yr BP	129	Ref.[90]	no	yes	Ref.[90,91]	Yes[47]	CC BY 4.0
WAIS Divide (WD)	-44 - beyond 7100 yr BP; gap between 2345 and 5380 yr BP	12 and 20 years in the most and less recent parts, respectively.	WD2014[35]	0.96	yes	Ref.[35]	Yes[51,52]	CC BY-NC 4.0

Table 1. Summary of key characteristics of ^{10}Be ice core data used in this study. The first five records (above the horizontal line in the middle of the table) are data prepared by the Orsay team. The next seven records (below the horizontal line in the middle of the table) are data prepared by other teams. The acronym corresponding to each record is indicated in parentheses in the first column.

For the Vostok site, measurements were performed following the same methodology every 50 cm on two adjacent cores, BH1 and BH2 respectively 178 m and 51 m deep (Fig. 3). Both cores were drilled in the clean sector 300 m west of the main station during the 1989-90 season using a thermal drill. Using BH1 ^{10}Be data, Raisbeck *et al.*[24] derived an age of ~7 ka at the bottom of this core.

For EPICA Dome C, continuous measurements have been performed from 7.7 m down to 51 m with either 1, 2 or 3 measurements along each 55 cm bag sample. For this study we have used 55 cm average values (Fig. 3). Based on the AICC time scale developed for this EPICA core[28,39] these ^{10}Be data cover ~1 ka. The ^{10}Be concentrations are higher at EPICA Dome C than at Old Dome C which (Table 2) is partly due to the lower accumulation at the EPICA site (by ~14%) despite the fact that the distance between the two drilling sites is only 50 km.

For Dome A measurements were performed on ice chips collected along a ~ 110 m shallow ice core (Fig. 3) drilled ~ 300 m from the summit during the 21st Chinese Antarctic Research Expedition (DA2005 ice core, CHINARE 21) in the 2004/05 austral summer[29]. Ice chips (~100 g) retained inside the drilling barrel were collected for each drilling run, weighed and transferred to plastic bottles together with the ^{9}Be carrier. The 135 melted samples were sent to Orsay for sample preparation (see above) and then measured at the Xi'an AMS Center. Zhang *et al.*[29] compared this ^{10}Be profile with the Δ^{14}C profile in dendrochronologically dated tree rings assuming different values of the mean accumulation rate. They first showed that the value of 1.6 g $H_2O/cm^2/yr$, suggested by Hou *et al.*[40] on the basis of the observed close off depth and a densification model[41], leads to a very poor match. They then tried larger accumulation values, in the range of those observed at Vostok and Dome C with similar ^{10}Be concentrations. They found the best fit with A = 2.31 g $H_2O/cm^2/yr$ and derived an age of ~3.2 ka at the bottom of this core. This choice was confirmed by similarities with the South Pole ^{10}Be over their common part. A similar value of 2.31 g $H_2O/cm^2/yr$ was previously derived for the period 1260 - 2005[42] (see also[43,44]).

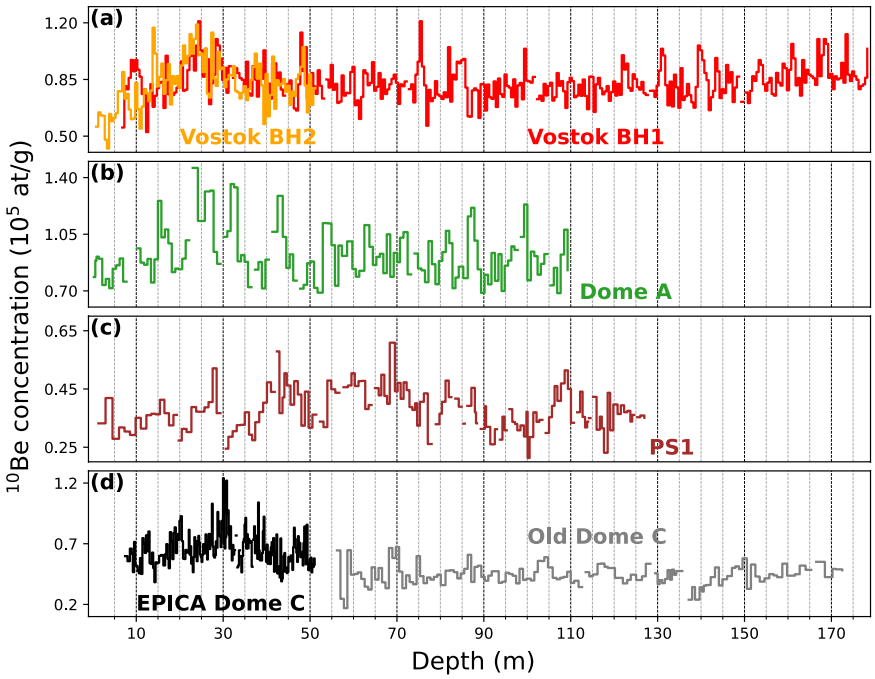

Fig. 3 ^{10}Be concentration with respect to depth measured along cores drilled at (**a**) Vostok (BH1 and BH2), (**b**) Dome A, (**c**) PS1, and (**d**) Dome C (Old Dome C and EPICA sites).

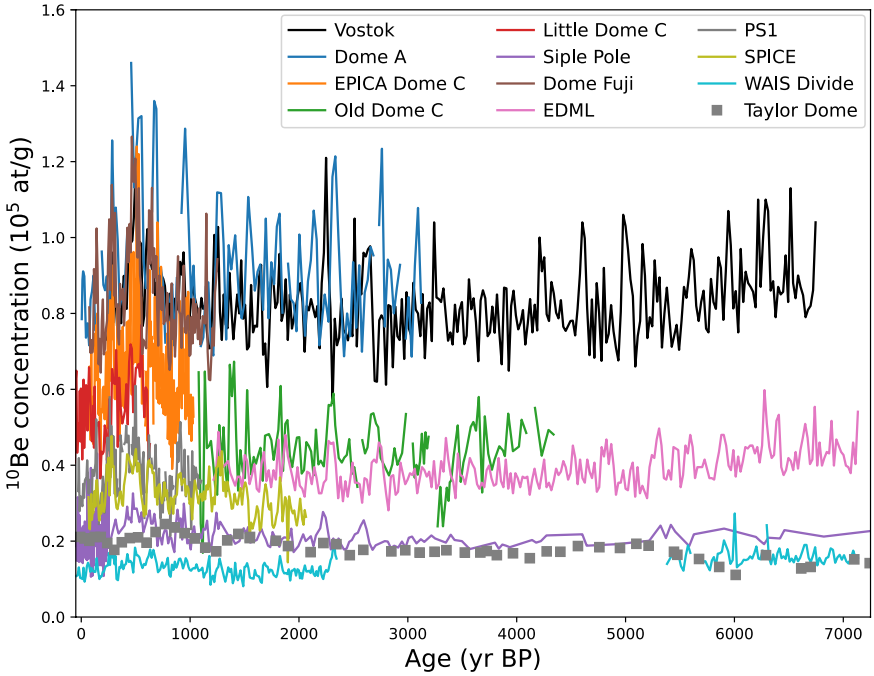

Fig. 4 ^{10}Be concentration at Vostok (combined BH1 and BH2 see below), EDML[45] on the AICC2012 timescale and WAIS Divide[35] on the WD2014 timescale. Data from old Dome C[19], Vostok[24], Dome F[49], South Pole (PS1[19] and SPICE[31]), Taylor Dome[47], Dome A[29], Siple Dome[46], and EPICA Dome C (this study) are plotted on their original timescales. For Little Dome C we have used the timescale inferred from the comparison of ^{10}Be profiles obtained at this site and at the Vostok site[50]. The Taylor Dome data, which are low resolution and discontinuous, are represented by data points (squares). All these data are expressed with respect to the NIST standard (except for Siple Dome, Taylor Dome and SPICE, see text).

^{10}Be ice core data from other sources. Our study - that we limit to the last seven millenia covered by our Vostok record - is also based on profiles obtained by other teams for five other Antarctic sites (Fig. 1). These include high resolution ^{10}Be profiles covering a large part of this period at EDML[45] where there is no data for the last millenia,

Site	Lat	Lon	Alt. obs.	Conc. obs.	Accu. obs.	Flux obs.	Alt. mod.	Conc. mod.	Accu. mod.	Flux mod.	Rconc	Rflux
Siple Dome	−81.65	−149.01	730	0.238	14.2	107.17	305	0.254	15.31	123.19	1.07	1.15
WD	−79.78	−112.13	1766	0.143	20.1	91.14	1628	0.233	17.36	128.39	1.63	1.41
PS1	−90.00	0.00	2800	0.390	8.72	107.84	2579	0.426	5.77	78.70	1.09	0.73
SPICE	−89.98	−98.15	2800	0.349	8.16	90.30	2579	0.336	5.33	56.78	0.96	0.63
EDML	−75.00	0.00	2892	0.399	6.28	79.46	2677	0.483	5.75	87.95	1.21	1.11
EDC	−75.06	123.21	3233	0.677	2.50	53.67	3165	0.575	2.97	54.13	0.85	1.01
LDC	−75.10	123.35	3233	0.590	2.31	43.22	3165	0.575	2.97	54.13	0.97	1.25
ODC	−74.39	124.10	3240	0.510	2.99	48.35	3121	0.468	4.84	71.78	0.92	1.48
Vostok	−78.47	106.80	3488	0.881	1.93	53.92	3414	0.817	1.73	44.83	0.93	0.83
Dome F	−77.32	39.70	3810	0.870	3.21	88.56	3666	0.690	2.57	56.16	0.79	0.63
Dome A	−80.37	77.37	4093	1.012	2.29	73.49	3879	0.770	2.50	61.16	0.76	0.83

Table 2. Observed (obs.) and ECHAM6.3-HAM2.3 modeled (mod.) values at the nearest grid cells for altitude (Alt, m), ^{10}Be concentration (Conc., 10^5 at/g), accumulation (Accu., g/cm^2/yr) and ^{10}Be flux (Flux, at/m^2/s). In the last two columns we have reported the modeled/observed ratio for ^{10}Be concentration (Rconc) and flux (Rflux). WD holds for Wais Divide, EDC for EPICA Dome C, LDC for Little Dome C and ODC for Old Dome C. For PS1, the ECHAM6.3-HAM2.3 modeled values correspond to the zonal mean at the latitude 88.57°S. For SPICE, the ECHAM6.3-HAM2.3 nearest grid cell are at the coordinates [88.57°S, 97.5°W] was taken.

and WAIS Divide[35] where data are missing between 2.3 and 5.3 ka. They are complemented by data covering also a large part of this period at Siple Dome[46] but with a discontinuous record over its older half, and at Taylor Dome[47] in this case with low resolution, and on a profile covering a shorter period at Dome F[48,49]. We also used ^{10}Be profiles available at two sites previously documented, Little Dome C (located in the Dome C area 40 km from the EPICA Dome C core and 82 km from old Dome C), for which ^{10}Be data have been measured on ice chips[50], and SPICE[32] at South Pole. The ^{10}Be records of WAIS Divide[51,52], SPICE[31], Dome F[53], Taylor Dome[47], and Siple Dome[46] are stored in public databases. As the EDML and Little Dome C records were used in previous publications but not published in a public database, requests to obtain these records were submitted to the respective authors of these ^{10}Be data (see Table 1). For EDML, data were provided only with respect to age after resampling with a 22-year time step. We thus have access to ^{10}Be profiles covering part of the Holocene at 9 different sites Dome C, Vostok, South Pole, Siple Dome, Taylor Dome, EDML, WAIS Divide, Dome F and Dome A. with multiple cores at three of these sites, Vostok (BH1 and BH2), Dome C area (Old Dome C, EPICA Dome C and Little Dome C) and South Pole (PS1 and SPICE).

To account for the fact that different laboratories use different different ^{10}Be/^{9}Be standards, we have performed a recalibration (by 0.89 for Dome F, 0.96 for WAIS Divide and Little Dome C and 0.91 for EDML) in order to have all these data expressed with respect to the NIST standard adopted at the Gif sur Yvette Tandetron (^{10}Be/^{9}Be = 2.68 • 10^{-11}); such recalibration has not been applied for Siple Dome, Taylor Dome and SPICE due to the lack of relevant information. All these data (from Orsay team plus the other sources) are reported on Fig. 4 with respect to time.

Δ^{14}C calibration curve IntCal20. For the ^{10}Be - ^{14}C correlation, the Δ^{14}C calibration curve IntCal20[34], which is available in open access at https://intcal.org/curves.html[54], was used.

Third-party softwares. The version 2.3.1 of the Match software[55] (https://lorraine-lisiecki.com/match.html) was used for the synchronizations with a graphical user interface on MATLAB R2024b release. To simulate the ^{14}C record based on ^{10}Be stack, a 12-box carbon cycle model[22], which is an hybrid of PANDORA[56] and the carbon cycle model used by Siegenthaler *et al.*[57], was used. These references[22,56,57] provide exhaustive information about the model geometry, specific equations and various parameters (carbon reservoir sizes, exchange fluxes and ^{14}C steady state). The model built with the STELLA software has performances and characteristics (impulse response function and Bode plot for attenuation and phase) in agreement with those of other models[58,59].

Data Records

The full dataset[60], including the compilation of ^{10}Be concentration data, their synchronisation on Vostok and PS1 ^{10}Be records, the stack calculations, the simulated Δ^{14}C time series, and the configuration files used for the synchronizations with Match protocol, is publicly available in the Figshare repository at https://doi.org/10.6084/m9.figshare.29623730. This dataset consists of seven excel files and one zip file, which are described below.

The ^{10}Be records prepared by the Orsay team (Vostok, Dome A, EPICA Dome C, old Dome C, and PS1; see the first subsection of Methods section and Table 1) are stored in the excel file named Be_holocene_data_orsay.xslx. The excel file contains a README tab with the references for each record and details on the structure of the file. The tab "Vostok (BH1 and BH2)" shows the ^{10}Be time series in Vostok BH1 and BH2, their merging, and their new age after synchronization on the Δ^{14}C calibration curve IntCal20. This age is used for the final stack. The tab "D14C derived from ^{10}Be Vostok" is the Δ^{14}C curve from ^{10}Be Vostok on its old (EGT) and its updated age scale after synchronization on IntCal20 Δ^{14}C time series. The tabs DA, EDC, ODC, and PS1 are the ^{10}Be data info from the ice cores measured by the Orsay team. The depth, original age, ^{10}Be concentrations, and the updated Δ^{14}C age scale after synchronization on Vostok's ^{10}Be data are shown.

The ^{10}Be records from other sources (Dome F, EDML, Little Dome C, Siple Dome, SPICE, Taylor Dome, and WAIS Divide; see the second subsection of Methods section and Table 1) are stored in the excel file named Be_holocene_data_others.xslx. As in the file Be_holocene_data_orsay.xslx, the references information, depth, original age, ^{10}Be concentrations, and the updated Δ^{14}C age scale after synchronization on Vostok's ^{10}Be data are shown. Both the original data values and the corrected ones after recalibration to NIST standard (noted with a "corr" notation) are shown.

The results of the synchronization of ^{10}Be records (except for Taylor Dome) on Vostok one are displayed in the excel file synchronisations_on_Vostok.xlsx. The Vostok's ^{10}Be data is displayed in the first five columns of each tab (one tab per site), including the mean depth, original age scale, updated Δ^{14}C age scale, ^{10}Be concentrations, and normalized ^{10}Be concentrations (by removing the mean and dividing by the standard deviation). In the subsequent columns, the original mean depth and age scales of the respective ^{10}Be records, their depth scale after synchronization on Vostok's ^{10}Be data, the updated Δ^{14}C age scale, the ^{10}Be concentrations relative to the NIST standard, their normalized values, and, if applicable, the measured ^{10}Be concentrations (for Dome F, WAIS Divide, Little Dome C, and EDML), are detailed. For Dome Fuji and Siple Dome, the synchronizations were made on the age scale due to the absence of depth information and the difficulty of performing this task using the depth scale, respectively. The resulting ^{10}Be stack derived from the synchronized ^{10}Be time series is shown in the file stack_calculation_on_Vostok.xlsx. For that, the ^{10}Be time series were resampled every 22 years, normalized through division by their mean ("resampling and flux calc" tab), and averaged at each interpolated age ("stack conc" tab). The same work has been performed with fluxes in the "stack flux" tab.

A similar synchronization exercise has been performed on the PS1 South Pole's ^{10}Be data for the SPICE, EPICA Dome C, Dome A, WAIS Divide, Dome F, Siple Dome, Little Dome C, and Vostok ^{10}Be records. The results are shown in the excel file synchronisations_on_PS1.xlsx. Similarly to the file synchronisations_on_Vostok.xlsx, the PS1's ^{10}Be data is displayed in the first four columns of each tab, including the mean depth, original age scale, ^{10}Be concentrations, and normalized ^{10}Be concentrations. In the subsequent columns, the original mean depth and age scales of the respective ^{10}Be records, their depth scale after synchronization on PS1's ^{10}Be data, the updated age scale, the ^{10}Be concentrations relative to the NIST standard, their normalized values, and, if applicable, the measured ^{10}Be concentrations, are detailed. The resulting ^{10}Be concentration stack derived from the synchronized ^{10}Be time series on PS1's ^{10}Be data is shown in the file stack_calculation_on_PS1.xlsx.

The Δ^{14}C time series based simulated with the 12-box ocean carbon cycle model by using Vostok and stack's ^{10}Be concentration time series are reported in the file C14_simulations.xlsx. A README describing each column of the sim_D14C result tab is included.

The configuration files to perform the synchronisations with the Match software are available in the zip file conf_file_match.zip.

Technical validation

^{10}Be profiles as a dating tool. *Applying the ^{10}Be - ^{14}C approach.* In this work, we have repeated the approach followed by Raisbeck *et al.*[24] with the following differences. First, we have combined the BH1 and BH2 records over their common part but excluding the top 15 meters (covering the last 250 years) as these cores were obtained using a thermal drill with an associated risk of modifying the ^{10}Be profiles over this upper part. Second, we have applied the Match protocol[55], a wiggle matching approach different from the one used by Raisbeck *et al.*[24]. This protocol was first applied to correlate the BH1 and BH2 ^{10}Be profiles over their common part - between 15 and 51 m depth - and derive an average profile over this part (Fig. 4). The match protocol appears quite accurate for this type of correlation as evaluated by the correlation to correspondences established from 6 volcanoes identified in both BH1 and BH2. The age difference between the two approaches has a mean value of 12 ± 8 years (1 σ).

The Match protocol was then applied to correlate the atmospheric ^{14}C record derived from the combined BH1 and BH2 ^{10}Be profiles using the 12-box carbon cycle model of Bard *et al.*[22], with the detrended IntCal20[34] ^{14}C tree ring record (Fig. 5). With an age of 7119 yr BP at 178 m depth (compared to 7160 for AICC), the resulting timescale, hereafter the Vostok *^{14}C timescale*, never differs by more than 60 years from the AICC2012 glaciological timescale currently used to interpret Vostok data (Fig. 6). It also is consistent with that estimated by Raisbeck *et al.*[24].

Correlating the ^{10}Be profiles between different sites. In a second step, we have derived a timescale for the other sites by synchronising the corresponding ^{10}Be profile with the Vostok one. To validate this approach, we have evaluated the accuracy of applying the match protocol to correlate ^{10}Be profiles by synchronizing the WAIS Divide and EDML ^{10}Be records and then comparing the result with an independent volcanic synchronisation established between these two cores[61]. For the periods over which ^{10}Be data are available at both sites, the two approaches (correlation using either ^{10}Be or volcanoes) compare quite well (Figure S1) with a small difference of -2 ± 11 yr (1σ).

Interestingly, the WAIS Divide core is absolutely dated by counting of annual layers observed in the chemical, dust and electrical conductivity records[35]. Over the past 2400 years, the uncertainty envelope of the WD2014 timescale is estimated to be smaller than 5 years. Prior to this period, the uncertainty on annual layer counting is estimated by inferring a ^{14}C record from ^{10}Be data and comparing it with the independent IntCal13 radiocarbon calibration curve[62]. Allowing for a possible offset of a couple of decades over the period covered by the brittle ice section between about 577 and 1300 m depth, the overall accuracy of layer counting is estimated to be better than 0.5%, e.g. a maximum of ~35 years at 7200 yr BP. For the period without ^{10}Be data at WAIS Divide (between 2339 and 5369 yr BP) we use the correlation between the Vostok and EDML ^{10}Be profiles and transferred it on to the WAIS Divide core based on the detailed and very precise correspondence established between EDML and WAIS Divide from volcanoes (Figure S1). We thus obtain a second absolute Vostok timescale, the *^{10}Be timescale*,

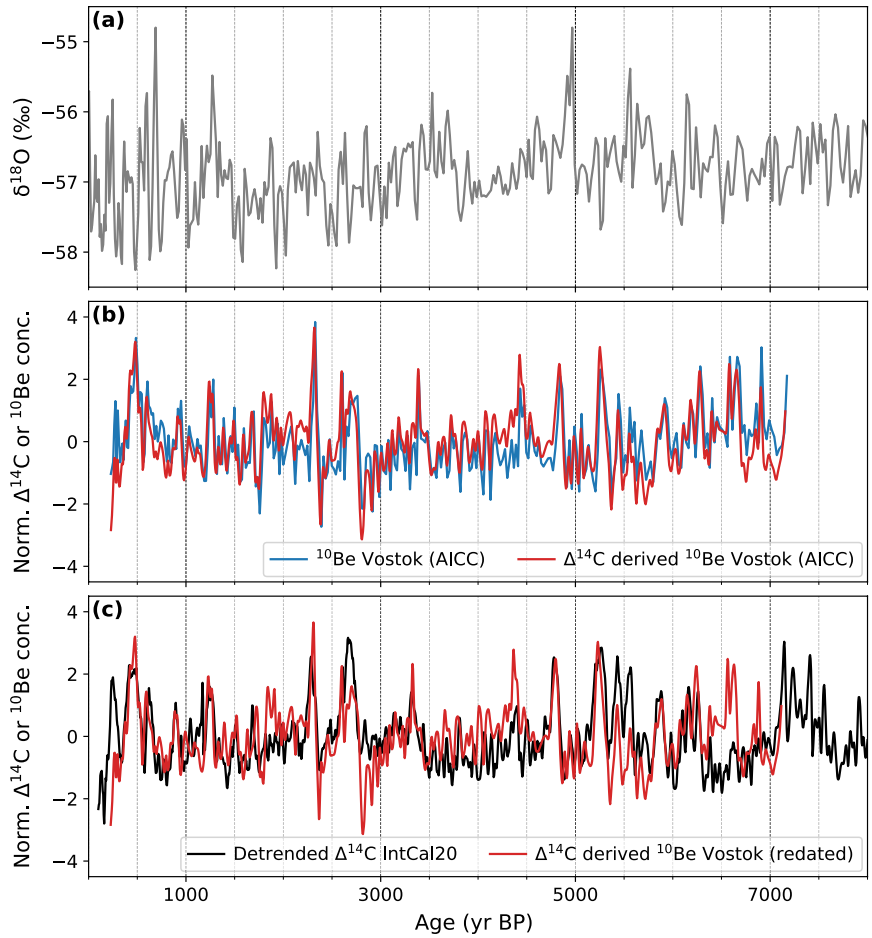

Fig. 5 (**a**) Oxygen-18 record (grey), a proxy of temperature change, measured on BH7 and BH8 cores located 100 m north of BH1[92]. (**b**) Combined BH1 and BH2 ^{10}Be record on the AICC timescale (in blue) and the Δ^{14}C derived from the ^{10}Be data (in red). (**c**) The same Δ^{14}C redated by matching (in red) with the detrended IntCal20 Δ^{14}C derived from tree rings (black) using the Match protocol. Time series in panels (**b**) and (**c**) are normalized by substracting the mean and dividing by the standard deviation.

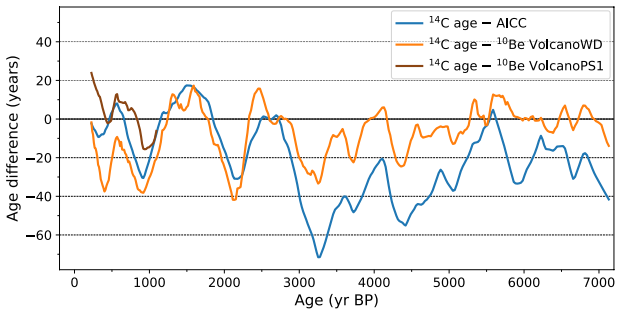

Fig. 6 Age difference between the ^{14}C timescale and 1) in blue: the AICC2012 timescale 2) in orange: the ^{10}Be timescale obtained applying the match protocol to correlate the Vostok ^{10}Be profile with profiles at WAIS Divide and EDML and 3) in brown: the same comparison performed for the PS1 core over the last 1100 years.

tied to WD2014 from present-day back to 7200 yr BP (Fig. 6). The two absolute timescales are in excellent agreement with an average difference of -9 ± 14 yr (1σ).

For the more recent part of this period - back to ~1100 yr BP - the PS1 ^{10}Be profile[19] is also absolutely dated with a precision ranging between 2 and 10 years thanks to the identification of 20 eruptions[38] followed by a slight revison of six of these eruptions[22,58]. Here also the agreement between the two approaches is very good (Fig. 6) with a difference of -3 ± 11 yr (1σ).

To sum up we can conclude that the accuracy of the absolute *^{14}C Vostok timescale* is probably better than ± 15 yr (1σ) as suggested from the comparison of its ^{10}Be profile with those available at WAIS Divide, EDML and South Pole.

^{10}Be fallout over Antarctica. *Geographical variability*. As shown in Fig. 4, there is between the different Antarctic sites a large spatial variability, up to a factor of 7, in the mean ^{10}Be concentration with higher values for low accumulation sites such as Vostok, Dome A and Dome F. This spatial variability over the Antarctic continent has already been documented generally from surface samples with a first approach dealing with the Dome C and Vostok sites[63]. For the first time, we have in our study an excellent coverage of the Antarctic continent with 5 sites well distributed over the East Antarctic Plateau, one inland in west Antarctica and 2 in coastal areas which offers the possibility to document the geographical variability of the ^{10}Be fallout over a large part of the Holocene.

As expected and already well documented[63], the snow accumulation effect can be partly compensated by calculating ^{10}Be fluxes. This requires to have access to snow accumulation and its variation through time. This is available for Vostok, EPICA Dome C and EDML sites for which age models have been developed deriving accumulation from temperature itself estimated for the isotopic composition of the ice[39]. For the WAIS Divide site, the accumulation is estimated combining layer counting with an ice flow model[64] with, due to the limited changes in climate during the Holocene, only small variations in accumulation during this period. Over the last 7000 years, its standard deviation is limited to 5% which justifies using a constant value for sites where there is no other estimate. We use estimates provided in literature for Siple Dome and Dome A while for South Pole, SPICE, Old Dome C and Little Dome C an average value was calculated directly based on the *^{10}Be timescale* developed for these ice cores. These accumulation values are reported for each core in the file stack_calculation_on_Vostok.xlsx.

Still, as illustrated in Figure S2 and Table 2, the range of variation of ^{10}Be fluxes is large - not far from a factor of 2 between Vostok and WAIS Divide - with lower ^{10}Be fluxes for the low accumulation sites. We also note that the EPICA Dome C flux is higher than in the two other cores drilled in the Dome C area, by respectively 23% (Little Dome C) and 14% (Old Dome C).

Numerous other sites have been investigated - e.g.[65] and references therein - with a good coverage in the Dronning Maud Land area thanks to a traverse upstream Kohnen station (the EDML drilling site) performed in 2006 by the Alfred Wegener Institute[65] and to data obtained during the austral summer 2007- 2008 by a swedish japanese team in its western part[66]. This expedition also allowed to extend the upstream Kohnen station german traverse roughly 400 km towards Dome F station[65]. More recently, in 2017 and 2019, the Japanese Antarctic Research Expeditions sampled sites along an inland traverse in eastern Dronning Maud Land[67]. The routes followed during these Dronning Maud Land traverses are indicated on Fig. 1 along with all the sites where ^{10}Be data are currently available.

These studies largely focus on the relationship between the ^{10}Be concentration and accumulation change or other parameters relative to the sampling site, latitude, elevation or distance from the coast[67]. The link with accumulation or related parameters is not surprising because, as for other aerosols, there is for ^{10}Be a combination of wet and dry depositions. The ^{10}Be concentration measured in the surface snow is the sum of its concentrations deposited by precipitation-related (wet deposition) and turbulent (dry deposition, which is inversely proportional to the accumulation) processes in the atmosphere. This results in a well documented linear relationship between ^{10}Be concentration and the inverse of the accumulation both in western[65] and eastern Donning Maud Land[67]. There is however a difference with the linear trend derived for the entire Antarctica[65] and in eastern Dronning Maud Land with a noticeable change in this linear trend at around 75°S (elevation 3500 m) as illustrated in Fig. 8 for the JARE traverse. This change is attributed to the dominance of wet deposition north of 75°S and of dry deposition south of this boundary[67].

In the following, we examine the ^{10}Be fallout variability (see Table 2 and Fig. 8, S2 and S3) as illustrated from the 11 dated cores (BH1 and BH2 being merged in one single record) covering part of the Holocene, thus excluding Taylor Dome (difficult to date). We use the average values of ^{10}Be concentration and flux calculated over the period from 237 to 985 yr BP (Table 2). When there is no data over this period (EDML and old Dome C) we take the value over the previous millennium and scale it using sites where data are available for the last two millennia (scaling factor 1.121). We proceed in the same way for Little Dome C where data are only available over a part of the last millenium (scaling factor 0.952). In turn, we avoid uncertainties associated with measurements covering too short periods with very large local associated variability[66] and the need for correction owing to different conditions of cosmogenic production variability[65].

For these 11 ^{10}Be records, we confirm the existence of a linear relationship between the ^{10}Be concentration and the inverse of the accumulation[65] from data covering shorter time periods with however a slightly higher slope (Figure S3). This higher slope results from the inclusion of Dome A data and significantly higher concentration than previously measured at Dome F which is confirmed by surface data obtained on samples collected during the JARE traverse[67].

Data-model comparison. The geographical distribution of these 11 cores allows a relevant comparison with simulations of ^{10}Be fallout using AGCMs. This is interesting because a simulation using the state-of-the-art ECHAM6.3-HAM2.3 AGCM has been recently published[36,68] combining this aerosol-climate model with the latest ^{10}Be production model (CRAC: Be[69]). This ensures that ^{10}Be fallout modeling is improved with respect to results previously based on simulations performed with the GISS model[70] and the previous ECHAM5 version[71,72] with lower resolution and less elaborated ^{10}Be production models.

The main purpose of this AGCM modeling - and this is also holds true for the study of Zheng *et al.*[36] - is to answer the question of whether the ^{10}Be deposition is proportional to global or local production rates,

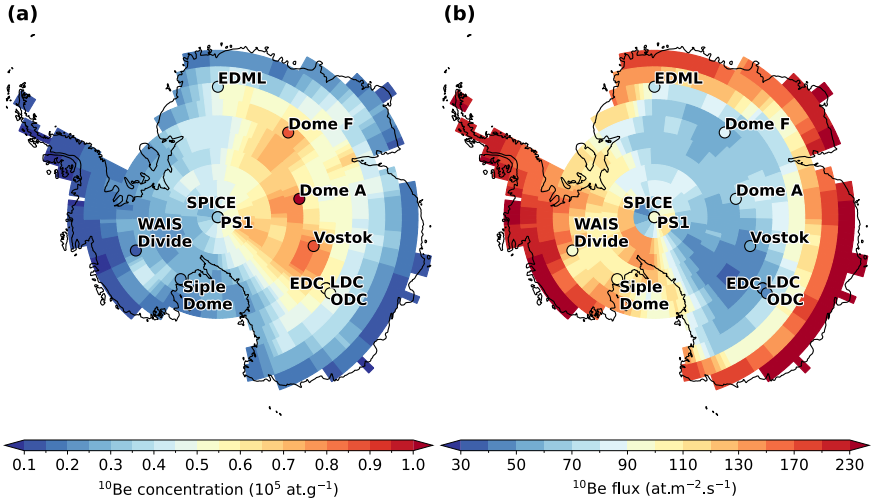

Fig. 7 Comparison between observed (colored circles) and ECHAM6.3-HAM2.3 results (colored background) for a) ^{10}Be concentration and b) ^{10}Be flux, respectively. The observed and modeled values for each station is reported on Table 2.

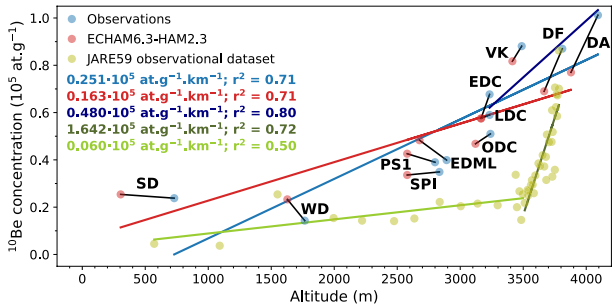

Fig. 8 ^{10}Be concentration with respect to the altitude for sites examined in this study with data (blue circles) and model results (red circles) and for sites along the JARE59 observational dataset (green circles). Regression lines are drawn for sites examined in this study (observed and modeled) and for JARE59 sites below and above 3500 m[67].

and in particular to investigate the "polar bias" debate. Hereafter, we will not discuss this important aspect but rather limit the use of the recent ECHAM6.3-HAM2.3 simulation results[68] to test the ability of such a modeling approach to correctly simulate the ^{10}Be fallout over Antarctica both for concentrations and fluxes. Observed and simulated concentrations and fluxes, together with their ratios are reported for each site in Table 2. Their geographical distribution is illustrated in Figs. 7a and 7b. Both the observed inland increase of ^{10}Be concentration and inland decrease for fluxes are well represented by the model. However there are some significant differences. This is not surprising given - as documented by[73] - the variability of aerosol transport processes between different sites which may be difficult to capture in a GCM simulation.

For concentrations, the comparison is satisfying (within ± 25%) for 10 out of the 11 ^{10}Be profiles for which data have been measured or estimated over the last millennium (period 237 - 985 yr BP when possible). Observed concentration value at WAIS Divide is not correctly captured by ECHAM6.3-HAM2.3 with a modeled value 63% too large. For fluxes, the average of simulated values for the 11 cores is in reasonable agreement with the observed average (73.2 and 81.9 at/m2/s, respectively). There is a good agreement (within ± 25%) between simulated and observed fluxes for Siple Dome, EDML, little Dome C and EPICA Dome C while simulated fluxes are ~30% too high for Old Dome C (due to too high modeled accumulation rate), WAIS Divide - where the too large simulated concentration is partly compensated by a higher simulated accumulation – PS1, and SPICE. Instead, simulated values are systematically lower (at 43 and 42%, respectively) than observed ones for the three highest elevation sites (>3400 m), Vostok, Dome A and Dome F. Finally, the comparison between Dome F and EPICA Dome C sheds light on a noticeable weakness of the simulation: while the measured ^{10}Be flux is 74% higher at Dome F than at EPICA Dome C, simulated values are quite similar (Table 2). Several reasons can explain such deficiency. The relatively coarse resolution means that the orography of Antarctic continent is smoothed compared to reality (Table 1), which influences the deposition processes, moisture transport and the precipitation patterns. Moreover, post-deposition effects such the redistribution of snow by the wind are not modeled. Also, the ECHAM6.3-HAM3.2 simulation has been performed for the period 2005-2013, whereas the

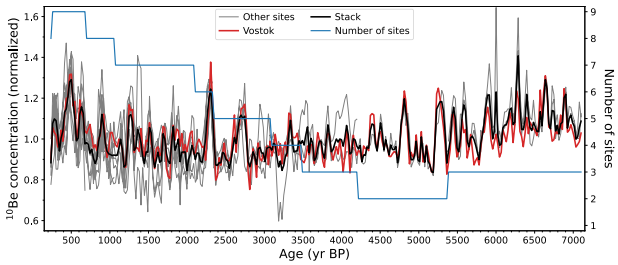

Fig. 9 22-yr time step ^{10}Be concentration time series (in grey) after matching with the Vostok profile (in red) using the Match protocol. The resulting stack is in black. Time series are normalized through division by their mean value.

observed values for the present study were considered for the period 237 to 985 yr BP, when the anthropogenic influence on climate was still limited.

In Fig. 8, ^{10}Be concentration are reported with respect to the altitude, both for sites examined in this study and along the JARE59 traverse. As a common characteristic, these two data sets exhibit a steeper increase for higher elevation sites. Focusing on the six sites on the East Antarctic Plateau (the three sites in the Dome C area, Vostok, Dome F and Dome A), there is a well observed ($r^2 = 0.80$) linear increase of 0.480 • 10^5 at.g^{-1} per km for the measured ^{10}Be concentrations (dark blue line in Fig. 8).

For simulated values, a weaker correlation ($r^2 = 0.57$) and a linear regression slope lower by 35% (0.320 • 10^5 at.g^{-1} per km) are found. This can be explained by the fact that the same grid cell encompassed the proximate station locations EDC and LDC, a consequence of the relatively coarse horizontal resolution of the ECHAM6.3-HAM2.3 simulation. Data obtained along the JARE59 route are organized along two different linear trends. A very low slope for the sites below 3500 m is found (0.060 • 10^5 at.g^{-1} per km). In contrast, for JARE59 sites above 3500 m, the slope is very steep (1.64 • 10^5 at.g^{-1} per km) and is much higher than for the 6 East Antarctic sites. Horiuchi *et al.*[67] concluded that the latitude of 75°S (or elevation of 3.5 km) is likely the most important boundary for ^{10}Be deposition along this JARE inland traverse route in eastern Dronning Maud Land with a deposition regime dominated by wet deposition north of 75°S and by dry deposition south of this latitude. These authors also evoked the seasonal enhancement of stratosphere-troposphere exchange with an associated increase of ^{10}Be concentration in austral summer.

Along this line, one can note that simulated fluxes are systematically underestimated for our high elevation sites located southward of 75°S (Fig. 7a, Vostok, Dome A and Dome F) while they are, for our other sites, correctly simulated or overestimated (Fig. 7a, WAIS Divide and Little Dome C). This could be explained by the difficulty of the ECHAM6.3-HAM2.3 simulation to account for such a boundary, the existence of which is thus somewhat supported by our data and their comparison with ECHAM6.3-HAM2.3 simulation. However, the ECHAM6.3-HAM2.3 simulation is overall very satisfying accounting correctly for the observed distribution of the ^{10}Be fallout over Antarctica. It would be thus quite justified to use this ^{10}Be version ECHAM6.3-HAM2.3 AGCM for other time spans such as glacial periods for which data are available at various sites (Dome C, Vostok, Dome F, EDML and WAIS Divide).

Towards a ^{10}Be stack for the last 7200 years. Following previous authors[45,58], we stacked the ^{10}Be records from the various sites. One advantage of stacking at moderate resolution (22 yr) multiple records with various sample spacings is to smooth out abrupt and large ^{10}Be spikes occurring during single years, such as extreme solar particle events[10–12] and volcanic eruptions[74,75]. To derive a stack record aiming to faithfully represent the average ^{10}Be fallout over Antarctica, it should be, in principle, better to combine ^{10}Be fluxes rather than concentration. However, there are additional uncertainties linked with estimates of the accumulation along the core, estimated through its link with water isotopes for Vostok, EPICA Dome C and EDML (AICC 2012 timescale[28]), derived by combining layer counting and a glaciological model at the WAIS Divide site[64] or limited to an average value due to the lack of data for the other sites. For all these reasons, we have calculated two stacks - one based on ^{10}Be concentrations and the other one based on ^{10}Be fluxes – which appears to be very similar.

We first calculated the mean value and standard deviation for each ^{10}Be concentration time series interpolated on a common time scale as described in the previous section. The standard deviation, expressed in % of the mean value, varies between 10% for Vostok and 16.7% for WAIS Divide considered as a single series. It was previously broken down into two series due to a large gap (2327-5385 yr BP). The shallow part would lead to a standard deviation of 14.7% and the bottom part to 11.5%. The average of relative standard deviations is 13.5%. Each time series was then normalized to its own average value, a procedure which retains its relative variability.

The 11 normalized time series were then averaged at each interpolated age, leading to the stack record (Fig. 9), which exhibits a standard deviation of 9.9% of the mean. This stack variability is thus somewhat smaller than observed for individual time series as illustrated by comparing this mean value with the time series from Vostok, the only site which covers the entire period. This is expected because observed variations are partly due to uncorrelated noise in the different time series (analytical uncertainties and genuine site-to-site differences).

It is difficult to quantify uncertainties of the stack record because the raw time series have neither the same length nor the same measurement resolution, even if time series are interpolated at the same ages. In particular, the total number of records drops to two during a millennium-long interval (5300-4200 yr BP) covered only

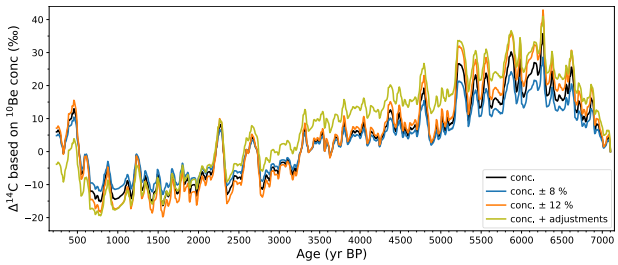

Fig. 10 Simulated $\Delta^{14}C$ time series (black) based on the ^{10}Be concentration stack used as an input of the 12-box model[22]. The blue and orange time series correspond to simulations with an enhanced variability of 8 and 12%, respectively, aiming to represent minimum uncertainties on the resulting $\Delta^{14}C$. The yellow curve corresponds to a simulation with the ^{10}Be stack with an enhanced long-term trend to take into account the polar bias for geomagnetic changes and a reduced high frequency variability to correct for the polar amplification of heliomagnetic changes[36]. An additional reduction of 5% of the variability has been applied to account for production sensibility differences for ^{14}C compared to ^{10}Be[69].

by the Vostok and EDML records. This makes it precarious to calculate uncertainties for each age based on a variable and sometimes low number of ^{10}Be concentrations. As a surrogate we use the average variability of the standard deviations calculated from the individual time series. The standard deviation of these values is 2%, which can be applied to the value at each age of the stack. In summary, the stack curve exhibits a variability (i.e., standard deviation) of 10% with an uncertainty range between 8 and 12%.

A similar stack has been calculated with the flux time series (Figure S4). Both concentration and flux stacks are very similar, which is due to limited variations of the ice accumulation over the last millennia. Furthermore, only some sites have independent estimations of the time variation of ice accumulation, whereas a constant accumulation is assumed at other sites (ODC, PS1, SPI, SD, DA, LDC). In that case, the relative variations of the flux are exactly the same as for the concentrations.

Due to the limited availability of ^{10}Be antarctic data for the Holocene, the focus of related studies has, long been limited to the last millenium with time series available at South Pole[19,22,23] and then Dome F[48,49,58]. Four additional time series covering this millenium are now available (Vostok, WAIS Divide, Dome A and EPICA Dome C). The mean value defined using these records is shown in Figure S5 after defining a common timescale based on correlation with the well dated South Pole ^{10}Be record. The two curves are quite similar but correlating with South Pole allows calculation of the mean value back to 1977 AD (instead of 1713 AD as in Figure S2). This millenium stack is very similar to the PS1 South Pole record[19] initially used to estimate solar irradiance over the last 1200 years[22,23].

Towards a simulated ^{14}C record based on ^{10}Be. Both stacks for ^{10}Be concentration and flux and their uncertainty ranges were used as input forcing curves for the 12 box-model[22]. Calculations start at 7100 yr BP with a model at preindustrial steady state (atmospheric $\Delta^{14}C = 0$). The ^{10}Be record is introduced as a perturbation of the cosmogenic production relative to its mean. Figure 10 shows the resulting simulated $\Delta^{14}C$ time series based on the ^{10}Be concentration. As expected, the simulations based on concentration and flux are similar, taking into account the estimated uncertainties (Figure S6).

All $\Delta^{14}C$ records are characterized by a long-term trend decrease of 20‰, notably between 7000 and 3000 yr BP. A similar multi-millennial trend exists in the ^{10}Be stacks, but it is less obvious because large centennial peaks are superimposed (Fig. 9). This contrast is a direct consequence of the different behaviors of ^{10}Be and ^{14}C, variations of ^{14}C being low-pass filtered by the carbon cycle (e.g. Figure 3 in[22]).

The observed $\Delta^{14}C$ record measured on tree-rings[34] is also characterized by a long-term trend over the Holocene. However, it is much steeper than the simulated trend based on ^{10}Be. Between 7000 and 2000 yr BP, atmospheric $\Delta^{14}C$ changes by about 100‰ and 20‰ in observed and simulated records, respectively. This long-term trend is linked to several cumulative phenomena as proposed in previous studies[30,76–79], in particular the geomagnetic field variations over the Holocene and the memory effect of the carbon cycle which integrates higher cosmogenic production before 7000 yr BP. Another source of variation are carbon-cycle changes that occurred during the Holocene as testified by atmospheric CO_2 variations[80].

The box-modeling approach assumes that ^{10}Be measured in polar ice is representative of the mean global cosmogenic production. This assumption is mainly based on the efficient mixing of ^{10}Be in the stratosphere, which partly homogenizes large production gradients. In reality, the atmosphere is incompletely mixed and correction factors have been suggested for a polar bias (e.g.[22,81]) which can also be evaluated with 3D models[36,65,70,82]. The further complexity is that this polar bias is different for the heliomagnetic and geomagnetic modulation of cosmogenic production: solar variations are enhanced at the poles whereas geomagnetic changes are subdued at high latitudes[20,22,83]. The exact magnitudes of polar biases linked to geomagnetic and solar modulations are still unsettled. Indeed, some model simulations indicate that ^{10}Be is well-mixed in the atmosphere[82], while other model experiments[65,70] show significant polar enhancement of solar variations and attenuation of geomagnetic changes in polar regions.

It is likely that centennial variations are due to the Sun whereas the multi-millennial trend is due to slow changes of the geomagnetic field[30,45,76,77,84,85]. As a first step to tackle these problems, we provide an additional

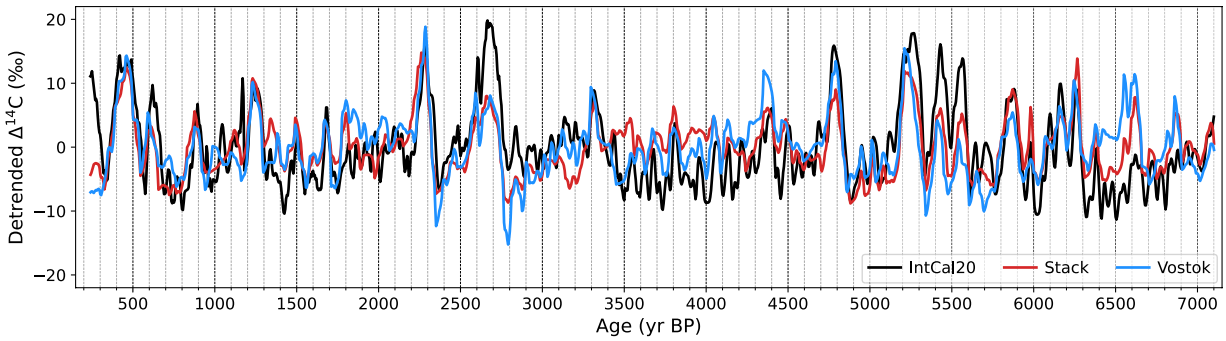

Fig. 11 Detrended $\Delta^{14}C$ modeled values obtained using either the ^{10}Be concentration stack (red curve) or the Vostok record alone (blue curve) with the detrended IntCal20 record (black curve).

$\Delta^{14}C$ simulation obtained by applying simple corrections to the ^{10}Be concentration stack: its long-term trend (as calculated over the 3-7 ka BP period) has been enhanced by 35% to take into account the maximum polar bias for geomagnetic changes and its high frequency variability has been reduced by 5% to correct for the maximum polar amplification evaluated for heliomagnetic changes[36]. An additional reduction of 5% of the variability has been applied to account for production sensibility differences for ^{14}C compared to ^{10}Be[69].

The corrected $\Delta^{14}C$ simulation is shown as a light-green line in Fig. 10. As expected, its long-term trend is enhanced by about 10‰ and its high frequency structures slightly reduced with respect to the standard case illustrated by the three other curves in Fig. 10. Nevertheless, the corrected $\Delta^{14}C$ record is close to the variability upper bound (±12%), suggesting that our first order uncertainties are reasonable.

Finally, we have in Fig. 11 compared the detrended $\Delta^{14}C$ simulation obtained using either the ^{10}Be stack or the Vostok record alone with the detrended IntCal20 record. The Pearson's correlation coefficient r and the Kendall's τ coefficient of the ^{10}Be stack with IntCal20 $\Delta^{14}C$ calibration curve are equal to 0.62 ($p = 6.89 \bullet 10^{-146}$) and 0.35 ($p = 1.29 \bullet 10^{-82}$), respectively. For the Vostok record alone with IntCal20 calibration curve, those coefficients are lower ($r = 0.50$ ($p = 1.29 \bullet 10^{-82}$) and $\tau = 0.28$ ($p = 6.12 \bullet 10^{-54}$), respectively). The difference between the two correlations is statistically significant at more than 99% according to a Steiger's Z test ($Z = 9.38$, $p\text{-}value = 8.99 \bullet 10^{-17}$). This suggests that the ^{10}Be stack provides a more representative global record than using Vostok alone.

Data availability

The ^{10}Be concentration data, their synchronisation on Vostok and South Pole ^{10}Be records, the stack calculations and the simulated $\Delta^{14}C$ time series are stored in seven excel files deposited in a Figshare database[60] at https://doi.org/10.6084/m9.figshare.29623730.

Code availability

The configuration files for the synchronizations with the Match software are publicly available in the same Figshare database[60] as a zip file (see the Data Records section). Python code to produce the figures are available in the GitHub repository at https://github.com/acauquoin/code_for_figures_10Be_Holocene/. The EDML-WAIS Divide link by the synchronization of their ^{10}Be records is also provided in the GitHub repository in the corresponding figure folders (Fig. 6 and S1).

Received: 8 August 2025; Accepted: 11 December 2025;
Published online: 10 January 2026

References

1. Chmeleff, J., von Blanckenburg, F., Kossert, K. & Jakob, D. Determination of the ^{10}Be half-life by multicollector ICP-MS and liquid scintillation counting. *Nuclear Instruments and Methods in Physics Research Section B: Beam Interactions with Materials and Atoms* **268**, 192–199 (2010).
2. Korschinek, G. *et al.* A new value for the half-life of ^{10}Be by Heavy-Ion Elastic Recoil Detection and liquid scintillation counting. *Nuclear Instruments and Methods in Physics Research Section B: Beam Interactions with Materials and Atoms* **268**, 187–191 (2010).
3. Raisbeck, G. M., Yiou, F., Fruneau, M. & Loiseaux, J. M. Beryllium-10 Mass Spectrometry with a Cyclotron. *Science* **202**, 215–217 (1978).
4. Golubenko, K., Rozanov, E., Kovaltsov, G. & Usoskin, I. Zonal Mean Distribution of Cosmogenic Isotope (^{7}Be, ^{10}Be, ^{14}C, and ^{36}Cl) Production in Stratosphere and Troposphere. *Journal of Geophysical Research: Atmospheres* **127**, e2022JD036726 (2022).
5. Usoskin, I. G. A history of solar activity over millennia. *Living Rev Sol Phys* **20**, 2 (2023).
6. Raisbeck, G. M., Yiou, F., Cattani, O. & Jouzel, J. ^{10}Be evidence for the Matuyama–Brunhes geomagnetic reversal in the EPICA Dome C ice core. *Nature* **444**, 82–84 (2006).
7. Raisbeck, G. M. *et al.* Evidence for two intervals of enhanced ^{10}Be deposition in Antarctic ice during the last glacial period. *Nature* **326**, 273–277 (1987).
8. Foukal, P. & Lean, J. An Empirical Model of Total Solar Irradiance Variation Between 1874 and 1988. *Science* **247**, 556–558 (1990).
9. Lean, J., Skumanich, A. & White, O. Estimating the Sun's radiative output during the Maunder Minimum. *Geophysical Research Letters* **19**, 1591–1594 (1992).
10. Mekhaldi, F. *et al.* Multiradionuclide evidence for the solar origin of the cosmic-ray events of AD 774/5 and 993/4. *Nat Commun* **6**, 8611 (2015).

11. Miyake, F. *et al*. ^{10}Be Signature of the Cosmic Ray Event in the 10th Century CE in Both Hemispheres, as Confirmed by Quasi-Annual ^{10}Be Data From the Antarctic Dome Fuji Ice Core. *Geophysical Research Letters* **46**, 11–18 (2019).
12. Miyake, F., Nagaya, K., Masuda, K. & Nakamura, T. A signature of cosmic-ray increase in AD 774–775 from tree rings in Japan. *Nature* **486**, 240–242 (2012).
13. Raisbeck, G. M., Yiou, F., Fruneau, M., Lieuvin, M. & Loiseaux, J. M. Measurement of ^{10}Be in 1,000- and 5,000-year-old Antarctic ice. *Nature* **275**, 731–733 (1978).
14. Raisbeck, G. M. *et al*. Cosmogenic ^{10}Be concentrations in Antarctic ice during the past 30,000 years. *Nature* **292**, 825–826 (1981).
15. Yiou, F., Raisbeck, G. M., Bourles, D., Lorius, C. & Barkov, N. I. ^{10}Be in ice at Vostok Antarctica during the last climatic cycle. *Nature* **316**, 616–617 (1985).
16. Raisbeck, G. M. *et al*. ^{10}Be deposition at Vostok, Antarctica during the last 50.000 years and its relationship to possible cosmogenic production variations during this period. in *The last deglaciation, absolute and radiocarbon chronologies* (eds Bard, E. & Broecker, W. S.) vol. NATO ASI Series, Subseries Global Environmental Change. I2 127–139 (Springer-Verlag, 1992).
17. Jouzel, J. *et al*. A Comparison of Deep Antarctic Ice Cores and Their Implications for Climate Between 65,000 and 15,000 Years. *Ago. Quat. res.* **31**, 135–150 (1989).
18. Beer, J. *et al*. Information on past solar activity and geomagnetism from ^{10}Be in the Camp Century ice core. *Nature* **331**, 675–679 (1988).
19. Raisbeck, G. M. *et al*. ^{10}Be and δ^2H in polar ice cores as a probe of the solar variability's influence on climate. *Phil. Trans. R. Soc. Lond. A* **330**, 463–470 (1990).
20. Raisbeck, G. M. & Yiou, F. Temporal Variations in Cosmogenic ^{10}Be Production: Implications for Radiocarbon Dating. *Radiocarbon* **22**, 245–249 (1980).
21. Raisbeck, G. M. & Yiou, F. ^{10}Be as a Proxy Indicator of Variations in Solar Activity and Geomagnetic Field Intensity During the Last 10,000 Years. in *Secular Solar and Geomagnetic Variations in the Last 10,000 Years* (eds Stephenson, F. R. & Wolfendale, A. W.) 287–296, https://doi.org/10.1007/978-94-009-3011-7_17 (Springer Netherlands, Dordrecht, 1988).
22. Bard, E., Raisbeck, G. M., Yiou, F. & Jouzel, J. Solar modulation of cosmogenic nuclide production over the last millennium: comparison between ^{14}C and ^{10}Be records. *Earth and Planetary Science Letters* **150**, 453–462 (1997).
23. Bard, E., Raisbeck, G., Yiou, F. & Jouzel, J. Solar irradiance during the last 1200 years based on cosmogenic nuclides. *Tellus B: Chemical and Physical Meteorology* **52** (2000).
24. Raisbeck, G. M. *et al*. Absolute Dating of the Last 7000 Years of the Vostok Ice Core Using ^{10}Be. *Mineralogical Magazine* **62A**, 1228–1228 (1998).
25. Jouzel, J. *et al*. Extending the Vostok ice-core record of palaeoclimate to the penultimate glacial period. *Nature* **364**, 407–412 (1993).
26. Parrenin, F., Jouzel, J., Waelbroeck, C., Ritz, C. & Barnola, J. Dating the Vostok ice core by an inverse method. *J. Geophys. Res.* **106**, 31837–31851 (2001).
27. Parrenin, F., Rémy, F., Ritz, C., Siegert, M. J. & Jouzel, J. New modeling of the Vostok ice flow line and implication for the glaciological chronology of the Vostok ice core. *J. Geophys. Res.* **109**, 2004JD004561 (2004).
28. Veres, D. *et al*. The Antarctic ice core chronology (AICC2012): an optimized multi-parameter and multi-site dating approach for the last 120 thousand years. *Clim. Past* **9**, 1733–1748 (2013).
29. Zhang, L., Raisbeck, G. M., Hou, S., Wu, Z. & Zhou, W. Estimating ice accumulation rate of a 109.91m ice core at Dome A, Antarctica, using ^{10}Be. in vol. International Partnerships in Ice Core Sciences (IPICS) Second Open Science Meeting (Hobart, Australia, 2016).
30. Nilsson, A. *et al*. Holocene solar activity inferred from global and hemispherical cosmic-ray proxy records. *Nat. Geosci.* **17**, 654–659 (2024).
31. Schaefer, J. South Pole ice Core ^{10}Be CE. U.S. Antarctic Program (USAP) Data Center, https://doi.org/10.15784/601535 (2022).
32. Casey, K. A. *et al*. The 1500 m South Pole ice core: recovering a 40 ka environmental record. *Annals of Glaciology* **55**, 137–146 (2014).
33. Pedro, J. B., Smith, A. M., Simon, K. J., van Ommen, T. D. & Curran, Ma. J. High-resolution records of the beryllium-10 solar activity proxy in ice from Law Dome, East Antarctica: measurement, reproducibility and principal trends. *Climate of the Past* **7**, 707–721 (2011).
34. Reimer, P. J. *et al*. The IntCal20 Northern Hemisphere Radiocarbon Age Calibration Curve (0–55 cal kBP). *Radiocarbon* **62**, 725–757 (2020).
35. Sigl, M. *et al*. The WAIS Divide deep ice core WD2014 chronology – Part 2: Annual-layer counting (0–31 ka BP). *Clim. Past* **12**, 769–786 (2016).
36. Zheng, M. *et al*. Modeling Atmospheric Transport of Cosmogenic Radionuclide ^{10}Be Using GEOS-Chem 14.1.1 and ECHAM6.3-HAM2.3: Implications for Solar and Geomagnetic Reconstructions. *Geophysical Research Letters* **51**, e2023GL106642 (2024).
37. Gillet, F. & Rado, C. A 180-metre core drilling at Dome C and measurements in the 905-meter drill hole. *Antarctic Journal of the United States* **14**, 101–102 (1979).
38. Delmas, R. J., Kirchner, S., Palais, J. M. & Petit, J.-R. 1000 years of explosive volcanism recorded at the South Pole. *Tellus B: Chemical and Physical Meteorology* **44**, (1992).
39. Bouchet, M. *et al*. The Antarctic Ice Core Chronology 2023 (AICC2023) chronological framework and associated timescale for the European Project for Ice Coring in Antarctica (EPICA) Dome C ice core. *Clim. Past* **19**, 2257–2286 (2023).
40. Hou, S., Li, Y., Xiao, C., Pang, H. & Xu, J. Preliminary results of the close-off depth and the stable isotopic records along a 109.91 m ice core from Dome A. *Antarctica. Sci. China Ser. D-Earth Sci.* **52**, 1502–1509 (2009).
41. Goujon, C., Barnola, J.-M. & Ritz, C. Modeling the densification of polar firn including heat diffusion: Application to close-off characteristics and gas isotopic fractionation for Antarctica and Greenland sites. *Journal of Geophysical Research: Atmospheres* **108** (2003).
42. Wang, Y. *et al*. Snow accumulation and its moisture origin over Dome Argus, Antarctica. *Clim Dyn* **40**, 731–742 (2013).
43. Hou, S., Li, Y., Xiao, C. & Ren, J. Recent accumulation rate at Dome A, Antarctica. *Chinese Sci Bull* **52**, 428–431 (2007).
44. Jiang, S. *et al*. A detailed 2840 year record of explosive volcanism in a shallow ice core from Dome A, East Antarctica. *Journal of Glaciology* **58**, 65–75 (2012).
45. Steinhilber, F. *et al*. 9,400 years of cosmic radiation and solar activity from ice cores and tree rings. *Proceedings of the National Academy of Sciences* **109**, 5967–5971 (2012).
46. Nishiizumi, K. & Finkel, R. C. Cosmogenic Radionuclides in the Siple Dome A Ice Core. U.S. Antarctic Program Data Center (USAP-DC), via National Snow and Ice Data Center (NSIDC), https://doi.org/10.7265/N5XK8CGS (2007).
47. Steig, E. J., Morse, D. L., Waddington, E. D., Stuiver, M. & Grootes, P. M. NOAA/WDS Paleoclimatology - Taylor Dome - High Resolution Oxygen Isotope and ^{10}Be Data. NOAA National Centers for Environmental Information, https://doi.org/10.25921/5THV-MC68 (2000).
48. Horiuchi, K. *et al*. Concentration of ^{10}Be in an ice core from the Dome Fuji station, Eastern Antarctica: Preliminary results from 1500 to 1810 yr AD. *Nuclear Instruments and Methods in Physics Research Section B: Beam Interactions with Materials and Atoms* **259**, 584–587 (2007).
49. Horiuchi, K. *et al*. Ice core record of ^{10}Be over the past millennium from Dome Fuji, Antarctica: A new proxy record of past solar activity and a powerful tool for stratigraphic dating. *Quaternary Geochronology* **3**, 253–261 (2008).
50. Nguyen, L. *et al*. The potential for a continuous ^{10}Be record measured on ice chips from a borehole. *Results in Geochemistry* **5**, 100012 (2021).
51. Welten, K. Cosmogenic Radionuclides in the WAIS Divide Ice Core. U.S. Antarctic Program (USAP) Data Center, https://doi.org/10.15784/600383 (2016).

52. Welten, K., Caffee, M. W., Nishiizumi, K. & Woodruff, T. E. Cosmogenic ^{10}Be in WAIS Divide Ice core, 1190-2453 m. U.S. Antarctic Program (USAP) Data Center, https://doi.org/10.15784/601466 (2021).
53. Horiuchi, K. *et al*. Dome Fuji, Antarctica Ice Core ^{10}Be Data 700-1900 CE. Arctic Data archive System (ADS), Japan (2008).
54. Ramsey, C. B. *et al*. Development of the Intcal Database. *Radiocarbon* **66**, 1852–1868 (2024).
55. Lisiecki, L. E. & Lisiecki, P. A. Application of dynamic programming to the correlation of paleoclimate records. *Paleoceanography* **17**, (2002).
56. Broecker, W. S. & Peng, T.-H. Carbon Cycle: 1985 Glacial to Interglacial Changes in the Operation of the Global Carbon Cycle. *Radiocarbon* **28**, 309–327 (1986).
57. Siegenthaler, U., Heimann, M. & Oeschger, H. ^{14}C Variations Caused by Changes in the Global Carbon Cycle. *Radiocarbon* **22**, 177–191 (1980).
58. Delaygue, G. & Bard, E. An Antarctic view of Beryllium-10 and solar activity for the past millennium. *Clim Dyn* **36**, 2201–2218 (2011).
59. Köhler, P., Knorr, G. & Bard, E. Permafrost thawing as a possible source of abrupt carbon release at the onset of the Bølling/Allerød. *Nat Commun* **5**, 5520 (2014).
60. Jouzel, J. *et al*. Beryllium 10 in Antarctica over the last seven millennia. FigShare https://doi.org/10.6084/m9.figshare.29623730 (2025).
61. Buizert, C. *et al*. Abrupt ice-age shifts in southern westerly winds and Antarctic climate forced from the north. *Nature* **563**, 681–685 (2018).
62. Reimer, P. J. *et al*. IntCal13 and Marine13 Radiocarbon Age Calibration Curves 0–50,000 Years cal BP. *Radiocarbon* **55**, 1869–1887 (2013).
63. Raisbeck, G. M. & Yiou, F. ^{10}Be in Polar Ice and Atmospheres. *A. Glaciology.* **7**, 138–140 (1985).
64. Fudge, T. J. *et al*. Variable relationship between accumulation and temperature in West Antarctica for the past 31,000 years. *Geophysical Research Letters* **43**, 3795–3803 (2016).
65. Elsässer, C. *et al*. Simulating ice core ^{10}Be on the glacial–interglacial timescale. *Clim. Past* **11**, 115–133 (2015).
66. Berggren, A.-M. *et al*. Variability of ^{10}Be and δ^{18}O in snow pits from Greenland and a surface traverse from Antarctica. *Nuclear Instruments and Methods in Physics Research Section B: Beam Interactions with Materials and Atoms* **294**, 568–572 (2013).
67. Horiuchi, K. *et al*. Spatial variations of ^{10}Be in surface snow along the inland traverse route of Japanese Antarctic Research Expeditions. *Nuclear Instruments and Methods in Physics Research Section B: Beam Interactions with Materials and Atoms* **533**, 61–65 (2022).
68. Zheng, M. *et al*. Modeling atmospheric transport of cosmogenic radionuclide ^{10}Be using GEOS-Chem 14.1.1 and ECHAM6.3-HAM2.3: implications for solar and geomagnetic reconstructions. FigShare, https://doi.org/10.6084/M9.FIGSHARE.24251884.V2 (2024).
69. Poluianov, S. V., Kovaltsov, G. A., Mishev, A. L. & Usoskin, I. G. Production of cosmogenic isotopes ^{7}Be, ^{10}Be, ^{14}C, ^{22}Na, and ^{36}Cl in the atmosphere: Altitudinal profiles of yield functions. *Journal of Geophysical Research: Atmospheres* **121**, 8125–8136 (2016).
70. Field, C. V., Schmidt, G. A., Koch, D. & Salyk, C. Modeling production and climate-related impacts on ^{10}Be concentration in ice cores. *Journal of Geophysical Research: Atmospheres* **111**, (2006).
71. Heikkilä, U., Beer, J., Jouzel, J., Feichter, J. & Kubik, P. ^{10}Be measured in a GRIP snow pit and modeled using the ECHAM5-HAM general circulation model. *Geophysical Research Letters* **35**, (2008).
72. Heikkilä, U., Beer, J. & Feichter, J. Modeling cosmogenic radionuclides ^{10}Be and ^{7}Be during the Maunder Minimum using the ECHAM5-HAM General Circulation Model. *Atmos. Chem. Phys.* **8**, 2797–2809 (2008).
73. Delmonte, B. *et al*. Ice core evidence for secular variability and 200-year dipolar oscillations in atmospheric circulation over East Antarctica during the Holocene. *Climate Dynamics* **24**, 641–654 (2005).
74. Baroni, M., Bard, E., Petit, J.-R., Magand, O. & Bourlès, D. Volcanic and solar activity, and atmospheric circulation influences on cosmogenic ^{10}Be fallout at Vostok and Concordia (Antarctica) over the last 60 years. *Geochimica et Cosmochimica Acta* **75**, 7132–7145 (2011).
75. Baroni, M., Bard, E., Petit, J.-R., Viseur, S. & Team, A. Persistent Draining of the Stratospheric ^{10}Be Reservoir After the Samalas Volcanic Eruption (1257 CE). *Journal of Geophysical Research: Atmospheres* **124**, 7082–7097 (2019).
76. Bard, E., Hamelin, B., Fairbanks, R. G. & Zindler, A. Calibration of the ^{14}C timescale over the past 30,000 years using mass spectrometric U–Th ages from Barbados corals. *Nature* **345**, 405–410 (1990).
77. Stuiver, M., Braziunas, T. F., Becker, B. & Kromer, B. Climatic, Solar, Oceanic, and Geomagnetic Influences on Late-Glacial and Holocene Atmospheric^{14} C/^{12} C Change. *Quat. res.* **35**, 1–24 (1991).
78. Cheng, H. *et al*. Atmospheric ^{14}C/^{12}C changes during the last glacial period from Hulu Cave. *Science* **362**, 1293–1297 (2018).
79. Heaton, T. J. *et al*. Radiocarbon: A key tracer for studying Earth's dynamo, climate system, carbon cycle, and. *Sun. Science* **374**, eabd7096 (2021).
80. Indermühle, A. *et al*. Holocene carbon-cycle dynamics based on CO_2 trapped in ice at Taylor Dome, Antarctica. *Nature* **398**, 121–126 (1999).
81. Adolphi, F., Herbst, K., Nilsson, A. & Panovska, S. On the Polar Bias in Ice Core ^{10}Be Data. *JGR Atmospheres* **128**, e2022JD038203 (2023).
82. Heikkilä, U., Beer, J. & Feichter, J. Meridional transport and deposition of atmospheric ^{10}Be. *Atmos. Chem. Phys.* **9**, 515–527 (2009).
83. Mazaud, A., Laj, C. & Bender, M. A geomagnetic chronology for antarctic ice accumulation. *Geophysical Research Letters* **21**, 337–340 (1994).
84. Usoskin, I. G., Solanki, S. K. & Korte, M. Solar activity reconstructed over the last 7000 years: The influence of geomagnetic field changes. *Geophysical Research Letters* **33**, 2006GL025921 (2006).
85. Roth, R. & Joos, F. A reconstruction of radiocarbon production and total solar irradiance from the Holocene ^{14}C and CO_2 records: implications of data and model uncertainties. *Clim. Past* **9**, 1879–1909 (2013).
86. Schwander, J. *et al*. A tentative chronology for the EPICA Dome Concordia Ice Core. *Geophysical Research Letters* **28**, 4243–4246 (2001).
87. Stenni, B. *et al*. A late-glacial high-resolution site and source temperature record derived from the EPICA Dome C isotope records (East Antarctica). *Earth and Planetary Science Letters* **217**, 183–195 (2004).
88. Brook, E. J. *et al*. Timing of millennial-scale climate change at Siple Dome, West Antarctica, during the last glacial period. *Quaternary Science Reviews* **24**, 1333–1343 (2005).
89. Winski, D. A. *et al*. The SP19 chronology for the South Pole Ice Core – Part 1: volcanic matching and annual layer counting. *Climate of the Past* **15**, 1793–1808 (2019).
90. Steig, E. J. *et al*. Synchronous Climate Changes in Antarctica and the North Atlantic. *Science* **282**, 92–95 (1998).
91. Steig, E. J. *et al*. Wisconsinan and Holocene Climate History from an Ice Core at Taylor Dome, Western Ross Embayment, Antarctica. *Geografiska Annaler: Series A, Physical Geography* **82**, 213–235 (2000).
92. Vimeux, F. *et al*. Holocene hydrological cycle changes in the Southern Hemisphere documented in East Antarctic deuterium excess records. *Climate Dynamics* **17**, 503–513 (2001).

Acknowledgements

We would like to thank participants in drilling, field work and ice sampling as well as the technical personnel at the Gif sur Yvette Tandetron. The study of Dome A was financially supported by "Partenariat Hubert Curien avec la Chine Program Cai Yuanpei (蔡元培) 2010-2012". EB is funded by ANR MARCARA. We also thank colleagues who have facilitated access to ^{10}Be and other data, Jürg Beer, Christo Buizert, Mark Caffee, Long Nguyen, Michael Sigl, Eric Steig and Kees Welten.

Author contributions

J.J. and G.R. initiated and coordinated this study. G.R. and F. Y. were responsible for the extraction, purification and preparation of ^{10}Be from ice core samples of Vostok, old Dome C, South Pole, and EPICA Dome C, and their measurement at the Gif sur Yvette Tandetron. V.L. and J.R.P facilitated the access to Vostok samples and to data used to exploit the corresponding ^{10}Be data. L.Z., S.H., W.Z, and Z.W prepared and measured the ^{10}Be samples of Dome A. L.Z. retrieved a funding for the Dome A ^{10}Be measurements. J.J. and G.R. collected the ^{10}Be data not prepared in Orsay Lab. J.J. and A.C. prepared and post-processed the ^{10}Be data for analyses and public database deposition. A.C. performed the synchronizations with the Match protocol software. E.B. performed the Δ^{14}C simulations with the 12-box model. A.C. created the FigShare database. J.J. wrote the first draft. A.C. made the figures. J.J., A.C., E.B., and G.R. revised substantially the manuscript. All co-authors participated in reviewing the manuscript.

Competing interests

The authors declare no competing interests.

Additional information

Supplementary information The online version contains supplementary material available at https://doi.org/10.1038/s41597-025-06444-0.

Correspondence and requests for materials should be addressed to J.J.

Reprints and permissions information is available at www.nature.com/reprints.

Publisher's note Springer Nature remains neutral with regard to jurisdictional claims in published maps and institutional affiliations.